Aquaculture Reports 45 (2025) 103090

Contents lists available at ScienceDirect

Aquaculture Reports

journal homepage: www.elsevier.com/locate/aqrep

Differential pathways to hepatic steatosis in fish: Divergent molecular mechanisms underlying high-carbohydrate versus high-lipid diet-induced lipid accumulation

Xiufei Cao [a], Yangyang Huang [a], Xiaoyu Chu [a], Xi Wang [a], Sunyuan Zheng [b], Xiaoli Shi [a], Xiaoe Xiang [a], Linghong Miao [c,d], Wenbin Liu [a], Guangzhen Jiang [a,*]

[a] Key Laboratory of Aquatic Nutrition and Feed Science of Jiangsu Province, National Experimental Teaching Center for Animal Science, College of Animal Science and Technology, Nanjing Agricultural University, No. 1 Weigang Road, Nanjing, Jiangsu 210095, China
[b] The Group of Nanjing University Academy of Environmental Planning & Design, No. 22 Hankou Road, Nanjing, Jiangsu 210008, China
[c] Wuxi Fisheries College, Nanjing Agricultural University, Wuxi 214081, China
[d] Key Laboratory for Genetic Breeding of Aquatic Animals and Aquaculture Biology, Freshwater FisheriesResearch Center, Chinese Academy of Fishery Sciences, Wuxi 214081, China

ARTICLE INFO

Keywords:
Hepatic steatosis
High-lipid diets
High-carbohydrate diets
VLDL secretion

ABSTRACT

High-carbohydrate and high-lipid diets are common high-energy diets that can reduce the protein consumption of fish and increase protein deposition in fish. However, long-term high-energy diets lead to liver steatosis and affect fish health. Fish utilize carbohydrates and fats differently, thus it is necessary to explore the differential effect of high-carbohydrate and high-lipid diets on abnormal liver fat deposition. Three isonitrogenous diets, including the control diets (CD), high-carbohydrate diets (HCD), and high-lipid diets (HFD), were formulated. Here, we reported that no differences were observed in the weight growth rate (WGR), condition factor (CF), and viscerosomatic index (VSI) of fish fed with high-energy diets compared to the control diets. High-lipid and high-carbohydrate diets increased the intraperitoneal fat ratio (IPF) and hepatosomatic index (HSI), respectively. *In vivo and in vitro*, biochemical parameters demonstrated that long-term high-energy diets caused liver damage in fish, increased liver or hepatocyte triglyceride content by more than 100 %, and inhibited VLDL secretion into plasma or medium. Oil red O staining also confirmed that high-energy diets significantly enhanced the liver lipid area of fish. In terms of ultrastructure, we found that high-carbohydrate diets increased the number of lipid droplets, while high-lipid diets increased the size and number of lipid droplets. Furthermore, high-lipid diets significantly up-regulated the gene or protein expressions related to fat synthesis, endoplasmic reticulum stress, and VLDL assembly *in vivo* and *in vitro*, while high-carbohydrate diets only up-regulated the expression of fat synthesis-related genes. These results indicated that high-carbohydrate diets induced hepatic fat deposition mainly through fat synthesis, but high-lipid diets promoted fat synthesis and inhibited VLDL secretion induced by endoplasmic reticulum stress. This study provides a molecular pathway for targeting hepatic steatosis caused by different energy diets.

1. Introduction

Fish can provide people with a variety of nutrients, especially high-quality protein. Aquatic products, including fish, have been the third largest source of dietary protein consumed by human beings around the world (Tacon and Metian, 2018). Due to the limitation of the wild capture fisheries, much of the current increase in fish consumption comes from aquaculture (Mizuta et al., 2022). The global population have already exceeded 8 billion in 2022, how to meet the nutritional requirements of such a large population has become a big challenge faced by government policymakers (Taagepera and Nemcok, 2024). As one of the most efficient agricultural sectors for protein production, the share of aquaculture in food supply will further increase. Especially for the underdeveloped third world countries, it is a good choice to get high quality fish protein at a relatively low price, which can be seen that aquaculture will be one of the most promising industries in the future

* Corresponding author.
E-mail address: jianggz@njau.edu.cn (G. Jiang).

https://doi.org/10.1016/j.aqrep.2025.103090
Received 28 June 2025; Received in revised form 14 August 2025; Accepted 5 September 2025
Available online 11 September 2025

(Tveteras et al., 2012).

Feed is the largest input in the aquaculture industry. Increase in fish consumption due to population growth and urbanization has driven up the price of feed ingredients. As we all know, the main sources of energy are protein, lipid and carbohydrate, which are also the most expensive part of the feed (Naylor et al., 2009). Compared to the terrestrial animals, aquatic animals require higher levels protein in their feeds to meet the demand of growth (Zhong et al., 2023). As the main protein ingredients, fishmeal is difficult to fully meet the development needs of aquaculture. A possible solution to promote growth and improve nitrogen retention is to increase the level of lipid and carbohydrate in the fish feed. The lipid in the feed can not only provide energy and spare protein, but also provide unsaturated fatty acids and phospholipids necessary for fish growth, and promote the absorption of fat-soluble vitamins (Watanabe, 1982). Carbohydrate is the most economical energy sources for aquatic feed due to its abundance and low cost. Apart from that, carbohydrate can improve the physical properties of the feed, such as pellet binding and water stability (Boujard et al., 2004; Li et al., 2010). However, long-term high-energy diets lead to liver steatosis and affect fish health. Fish utilize carbohydrates and fats differently, thus it is necessary to explore the differential effect of high-carbohydrate and high-lipid diets on abnormal liver fat deposition.

Under the intensive aquaculture model, the lipid and carbohydrate content of feeds has been substantially increased in order to improve economic returns. However, excess lipid and carbohydrate in the diet led to the development of fatty liver, which ultimately impaired the growth performance of fish (Lu et al., 2013; Xie et al., 2017; Cao et al., 2019). Currently, lipid metabolism is an important research hotspot for evaluating the ability of fish to utilize carbohydrate and lipid. The secretion of very low-density lipoprotein (VLDL) is one of the key determinants of lipid content in the liver (Fisher, 2012). Studies on rats, fish and people has shown that the main symptoms of fatty liver are increased fat synthesisthe and inhibition of lipoprotein secretion (Chen et al., 2022; Karavia et al., 2013; Spaulding et al., 2023). The formation of VLDL generally consists of two steps, the first step is the formation of VLDL precursors from small amounts of lipids and apolipoprotein B (ApoB) with the assistance of microsomal triglyceride transfer protein (MTTP), the second step is the binding of VLDL pre cursors with large amounts of lipid to form mature VLDL particles that are rich in large amounts of lipid (Ye et al., 2009). Studies in mice have shown that the large amount of lipid required for VLDL lipidation to mature can come directly from lipid droplets (Ye et al., 2009). Lipid droplets are a highly dynamic organelle in hepatocytes storing neutral fat (Li et al., 2012).

Our previous study has found that high lipid diet activate the endoplasmic reticulum stress-related IRE1/XBP1 pathway, and finally induced the obstacles of liver lipid secretion (Cao et al., 2019). Similar conclusions have been verified for other fish species (Fang et al., 2021). However, it is not known how the effects of high carbohydrate and high lipid diets differ on fat synthesis and VLDL secretion in fish. *Megalobrama amblycephala* is one of the famous herbivorous carp fish in China, and its production in 2023 has reached 738727 tons. Due to its relatively low HSI compared to other teleost fish, it is also a good model for studying lipid metabolism. Thus, in this study, we investigated the effects of high carbohydrate and high lipid diets on endoplasmic reticulum stress, VLDL secretion, and lipid droplet formation in *Megalobrama amblycephala*.

2. Materials and methods

2.1. Ethical statement

This study has been approved and strictly supervised by the Animal Care and Use Committee of Nanjing Agricultural University (Nanjing, China; permit number: SYXK (Su) 2011–0036).

2.2. Animals, diets, farming management, and sample collection

A feeding trial was carried out at Pukou Fisheries Research Station (Nanjing, China). The three diets, including the control diets (CD, 6 % lipid and 28 % carbohydrate), high-carbohydrate diets (HCD, 40 % carbohydrates), and high-lipid diets (HFD, 11 % lipids), were made with reference to our previous study (Huang et al., 2022). All ingredients were finely ground and processed through a 60 mm mesh. After ingredients were weighed and well mixed, the diet was prepared into particles with a particle size of 2 mm and stored at −20 ℃. All diets were stored at −20℃ in sealable bags until used. Juvenile blunt snout bream for the experiment were purchased from a local farm in Wuhan (Hubei, China). These fish were domesticated for two weeks with commercial feed (30 % crude protein, 6 % crude fat) provided by Tongwei Group China (www.tongwei.com). A total of 360 healthy juvenile fish (19.56 ± 0.17 g) were randomly divided into 18 floating net cages (2 m × 1 m × 1 m; length × width × height) with six replicates per group at a rate of 20 fish/cage. The fish were fed with experimental diets three times a day at 8:00, 12:00, and 16:00. During the 11 weeks feeding trial, dissolved oxygen was remained > 5.0 mg/L; the temperature of water ranged from 28 to 34°C; pH was 7.1–7.4; and total ammonia nitrogen and nitrite were remained lower than 0.4 and 0.01 mg/L.

All experimental fish were euthanized with MS-222 (100 mg/L, Cat#886–86–2, Sigma-Aldrich, USA) prior to biological sampling. The total number and weight of fish in each cage were recorded. Three fish per cage were randomly selected for biometric analysis, with standard length and body weight recorded. Blood samples collected via caudal venipuncture were immediately centrifuged (3000 *g*, 4°C, 10 min) to separate plasma, which was snap-frozen in liquid nitrogen and stored at −80°C. Visceral mass, intraperitoneal fat, and liver tissue were dissected and weighed. Liver samples were subsequently flash-frozen in liquid nitrogen and maintained at −80°C for biochemical analyses, histological stain, qRT-PCR, and western blot.

2.3. Biochemical parameters

The biochemical parameters of plasma, liver, medium, and hepatocytes were performed with the commercial kits. Aspartate aminotransferase activity (AST), alanine aminotransferase activity (ALT), very low-density lipoprotein (VLDL), and triglycerides (TG) content were measured using commercial kits (Cat#C010–2–1, Cat#C009–2–1, Cat#H249–1–1, and Cat#A110–1–1, respectively) from Nanjing Jiancheng Bioengineering Institute (Nanjing, China), following the manufacturer's instructions. Before measuring, blood was collected through the tail vein of the fish and centrifuged at 3000 *g* for 10 min at 4℃ to obtain plasma. The liver was mixed with cooled PBS at a 1: 9 (weight (g)/volume (mL)) rate. The supernatant was obtained for analysis of biochemical parameters after the liver and PBS mixture was homogenized and centrifuged at 2500 *g* for 10 min at 4℃. After fish primary hepatocytes were incubated for 12 h using either 40 mM glucose (GLU) or 0.4 mM oleic acid (OA), the medium was collected and centrifuged at 1000 *g* for 5 min at 4℃. However, hepatocytes were mixed with cooled RIPA lysate buffer (Cat#P0013B, Beyotime, China). The supernatant was obtained for analysis of biochemical parameters after the mixture was crushed and centrifuged at 2500 *g* for 10 min at 4℃. The enzyme activities of AST and ALT in plasma were measured at 510 nm and 505 nm via the formation of 2,4-dinitrophenylhydrazone. VLDL content in plasma and medium was measured at 450 nm using the double antibody sandwich ELISA method. TG content in the liver and hepatocytes was measured at 500 nm via the formation of quinone compounds.

2.4. Histological analysis

Liver samples were fixed in 4 % formaldehyde, then dehydrated and embedded in paraffin wax. Three micron-thick slices were prepared and stained with oil red O. Then, they were examined and photographed by

Nikon Microscope Eclipse Ni (Nikon Corporation, Tokyo, Japan). For each dietary group, liver samples from 4 fish were analyzed. From each fish, 3 sections were prepared. The relative areas of the lipid droplets in liver sections stained with oil red O were measured using Image J Pro 1.52 software (National Institutes of Health, Bethesda, USA).

2.5. Ultrastructure of the liver

The samples of liver were fixed in 2.5 % glutaraldehyde for 24 h and then fixed with 1 % osmium tetroxide (O_sO_4), stored at 4°C for 1 h. Sections were embedded in epoxy resin Epon812, cut into 70-lm-thick sections with a RMC Power Tome XL microtome, stained with uranyl acetate and lead citrate, and examined under a Hitachi H-7650 (Hitachi, Tokyo, Japan) transmission electron microscope. The diameter of lipid droplet was measured using Image J Pro 1.52 software (National Institutes of Health, Bethesda, USA).

2.6. The culture and treatment of fish primary hepatocytes

Primary hepatocytes were isolated from experimental fish using standardized protocols (Cao et al., 2019). Briefly, the fish were surface-disinfected with 75 % ethanol and euthanized by exsanguination. Liver tissue (2 g) was aseptically excised and mechanically dissociated into a single-cell suspension through 20 mL collagenase IV digestion (1 mg/mL). The resultant homogenate was filtered through a 100-μm nylon mesh and subjected to differential centrifugation (300 *g*, 10 min, 4°C). Pelleted hepatocytes underwent three PBS washing cycles before resuspension in complete medium: DMEM/F12 supplemented with 10 % fetal bovine serum (FBS), 1 mM L-glutamine, 100 IU/mL penicillin, and 100 μg/mL streptomycin. Cells were plated at 1×10^6 cells/mL in collagen-coated 6-well plates and maintained at 28°C in 5 % CO_2 for 48 h to establish confluent monolayers. Following serum starvation for 6 h, cells were exposed to experimental conditions containing 0.4 mM oleic acid (OA, Matreya LLC, Cat#1022, USA) complexed with fatty acid-free BSA and 40 mM D-glucose (Sigma-Aldrich, Cat#G7021, USA) for 12 h based on previous studies (Cao et al., 2019; Dong et al., 2024). Subsequently, cells were lysed in TRIzol reagent for subsequent biochemical parameters, RNA isolation, and qRT-PCR analysis of target gene expression.

2.7. RNA extraction and quantitative real-time PCR analysis (qRT-PCR)

The total RNA of the liver and hepatocytes was extracted by using Trizol (Invitrogen, USA). Following the manufacturer's instructions, cDNA was produced from DNase-treated RNA using the ExScript RT-PCR kit. Primer sequences for the target genes were manufactured by Shanghai Generay Biotech Co., Ltd. (Shanghai, China), which are showen in Table 1. And then, qRT-PCR was performed by using SYBR Green Pro Taq HS Premix (Cat#AG11701, Accurate Biology, China). The qRT-PCR of target genes was conducted in the CFX96 Touch Real-Time PCR Detection System (Bio-Rad, USA) and carried out in a final reaction volume of 20 μl containing 10 μl of 2 × SYBR Green Pro Taq HS Premix, 0.4 μl (10 μM) of each pair primer, 5.6 μl of DEPC, and 4 μl of cDNA template. Elongation factor 1α (EF1α) was used as an internal control. The relative expression of target genes was evaluated according to the $2^{-\Delta\Delta CT}$ method.

2.8. Western blot analysis

Liver tissue was lysed with RIPA lysis buffer (Cat#P0013B, Beyotime, China) containing protease and phosphatase inhibitor (Thermo, USA). The concentrations of protein were quantified using a BCA protein assay kit (Cat#P0009, Beyotime, China). The protein was heat-denatured, separated by SDS-PAGE electrophoresis, and transferred to a 0.45 μm polyvinylidene fluoride (PVDF) membranes (Millipore, Massachusetts, USA). The member was blocked with 5 % fat-free dry milk in TBST buffer for 1 h at room temperate and incubated with primary antibody overnight at 4°C. The membrane was then incubated with the horseradish peroxidase (HRP)-conjugated secondary antibodies for 2 h at room temperature. The primary antibodies were ADRP (Cat#ab52356, abcam, UK), MTTP (Cat#A1746, ABclonal, China), GRP78 (Cat#A0241, ABclonal, China), IRE1 (Cat#A17940, ABclonal, China), p-IRE1 (Cat#AP0878, Abclonal, China), β-actin (Cat#AC026, ABclonal, China). Finally, Bands were visualized by ECL reagents (Cat#P0018S, Beyotime, China). The intensity of the target band was quantified using Image J Pro 1.52 software (National Institutes of Health, Bethesda, USA). The protein expression levels of GRP78, ADRP, and MTTP were normalized to β-actin as an internal control, while phosphorylated IRE1 (p-IRE1) levels were expressed relative to total IRE1 protein.

2.9. Statistical analysis and calculations

Data were analyzed by one-way ANOVA using the SPSS 19.0 software (IBM, USA) for Windows. Significant differences between groups were determined by the Tukey multiple range test, after data were tested

Table 1
Primer sequences for quantitative real-time PCR.

Gene	Primer sequences (5′ - 3′)		Product size (bp)	Accession number	Amplification efficiency
dgat1	F	GAAATCAGACACGCCAAAGC	176	XM_048203124.1	0.98
	R	CGTGGGAAATTCAGCTCGTA			
fatp	F	CTTCTTCCTGGTGGCATCCT	208	XM_048188190.1	0.95
	R	TGGGTTCAACAGTCGCATTCT			
fabp	F	CTCGTTCACTGTGGGTGAGG	95	XM_048189882.1	0.97
	R	ACACCGTCAGCTTATTCCCG			
mttp	F	CGCTTTCTGTACGCATGTGG	103	KM980090.1	1.01
	R	CCTTAATGTCTGGGCTGCCA			
grp78	F	CGTTCAGGCTGGAGTTCTGT	175	XM_048180391.1	0.98
	R	GTTGTCAGAAGCGGTGGAGA			
ire1	F	AGAGACCCTCGGCTGACAGA	139	MG763105.1	0.98
	R	CCTCTCTCCAGCTGCCTCAC			
xbp1s	F	GTGGTGAGCGAGGAGAGCAT	182	MG763107	0.96
	R	GAGGCGTCGGAGAGGAAGTC			
adrp	F	AAGACGGTGGTTAGCAGTGG	214	XM_048161142.1	0.98
	R	GAGACCCCAGTCGAACGAAG			
ef1α	F	CAAGGAAGTCAGCGCCTACA	129	XM_048201754.1	0.98
	R	CATCCCTTGAACCAGCCCAT			

Notes. *dgat1*, diacylglycerol O-acyltransferase 1; *fatp*, fatty acid transport protein; *fabp*, fatty acid binding protein; *mttp*, microsomal triglyceride transfer protein; *grp78*, glucose regulated protein 78; *ire1*, inositol requiring enzyme 1; *xbp1s*, spliced X box-binding protein 1; *adrp*, adipose differentiation-related protein; *ef1α*, elongation factor 1α.

for equality of variances with Levene's test. The level of significance was set at $P < 0.05$. All results were expressed as mean ± SEM.

3. Results

3.1. Growth performance and somatic parameters

There were no significant differences in weight growth rate (WGR), condition factor (CF), and viscerosomatic index (VSI) among experimental groups ($P > 0.05$) (Table 2). Compared to CD, Intraperitoneal fat ratio (IPF) was significantly increased in fish fed with HLD and hepatosomatic index (HSI) was significantly increased in fish fed with HCD ($P < 0.05$) (Table 2).

3.2. Biochemical parameters in vivo and in vitro

The enzyme activities of aspartate aminotransferase (AST) and alanine aminotransferaseand (ALT) were significantly increased in plasma of fish fed with HCD and HLD ($P < 0.05$) (Fig. 1A–B), while plasma very low-density lipoprotein (VLDL) content was inhibited in fish fed with HCD and HLD ($P < 0.05$) (Fig. 1C). In addition, the content of liver triglycerides (TG) was increased in fish fed with HCD and HLD ($P < 0.05$) (Fig. 1D). Fish primary hepatocytes were incubated for 12 h using either 40 mM glucose (GLU) or 0.4 mM oleic acid (OA) to establish *in vitro* models of high-carbohydrate and fat levels (Fig. 1E). Consistent with results *in vivo*, high dose of glucose and oleic acid reduced the VLDL content in medium and increased the TG content in hepatocytes ($P < 0.05$) (Fig. 1F–G).

3.3. Analysis of liver morphology and ultrastructure

Oil red O staining was used to assess hepatic lipid deposition in fish fed with different energy diets. The neutral lipids of the liver were stained red (Fig. 2A). The area of lipids in the liver of fish fed with HCD and HLD was higher than that of fish fed with CD ($P < 0.05$) (Fig. 2B). In addition, the ultrastructure of hepatocytes was observed using transmission electron microscope. Compared to CD, HCD promoted the number of lipid droplets and HLD increased the size and number of lipid droplets (Fig. 2C). Indeed, the diameter of lipid droplets was increased 2.5-fold and 5.7-fold in fish fed with HCD and HLD, respectively ($P < 0.05$) (Fig. 2D).

3.4. Gene expression in vivo

Gene expression was measured to assess endoplasmic reticulum stress and lipid metabolism in fish fed with high-energy diets. The high-lipid diets promoted the expressions of ER stress-related genes, including glucose regulated protein 78 (*grp78*), inositol requiring enzyme 1 (*ire1*), and spliced X box-binding protein 1 (*xbp1s*), while high-carbohydrate diets did not ($P < 0.05$) (Fig. 3A—C). In addition, the gene expressions of microsomal triglyceride transfer protein (*mttp*) and adipose differentiation-related protein (*adrp*) were increased in the liver of fish fed with HCD compared to CD, but decreased in the liver of fish fed with HLD compared to HCD ($P < 0.05$) (Figs. 3D and 3H). In terms of fat synthesis, the gene expressions of fatty acid transport protein (*fatp*), fatty acid binding protein (*fabp*), and diacylglycerol acyltransferase 1 (*dgat1*) were increased in the liver of fish fed with HCD or HLD compared to CD ($P < 0.05$) (Fig. 3E-3G). Furthermore, the expression of the *dgat1* gene was significantly upregulated in the hepatic tissue of fish fed with HLD compared with those fed with HCD ($P < 0.05$) (Fig. 3G).

Table 2
Growth performance and somatic indexes of *Megalobrama amblycephala* fed with the experimental diets.

	CD	HCD	HLD
WGR (%)	423.45 ± 9.36	426.28 ± 8.47	410.49 ± 22.09
CF (g cm^{-3})	2.27 ± 0.12	2.27 ± 0.03	2.21 ± 0.03
VSI (%)	6.31 ± 0.14	6.62 ± 0.27	6.9 ± 0.12
IPF (%)	2.09 ± 0.09^{b}	2.31 ± 0.13^{b}	2.94 ± 0.11^{a}
HSI (%)	1.02 ± 0.03^{b}	1.14 ± 0.04^{a}	0.9 ± 0.03^{c}

Notes. Data were presented as mean ± SEM (one-way ANOVA, n = 4). Values with the same uppercase letter or absence of superscripts are not significantly different among the groups ($P > 0.05$). Weight growth rate (WGR, %) = (Final body weight − Initial body weight)/Initial body weight × 100. Condition factor (CF, g/cm^3) = 100 × Final body weight (g) / Final body length $(cm)^{3.}$ Viscerosomatic index (VSI, %) = Viscerosomatic weight (g) / Body weight (g)× 100. Intraperitoneal fat ratio (IPF, %) = Intraperitoneal fat weight (g) / Body weight (g) × 100. Hepatosomatic index (HSI, %) = Liver weight (g) / Body weight (g) × 100

3.5. Gene expressions in vitro

In vitro, gene expression in hepatocytes was measured to assess endoplasmic reticulum stress and lipid metabolism after hepatocytes were exposed to 40 mM D-glucose (GLU) and 0.4 mM oleic acid (OA) for 12 h. The expression of ER stress-related gene, including *grp78*, *ire1*, and *xbp1s*, was significantly upregulated in hepatocytes treated with OA ($P < 0.05$) (Fig. 4A–C). However, the expression of the *grp78* and *ire1* genes was significantly downregulated in hepatocytes treated with GLU ($P < 0.05$) (Figs. 4A and 4B). In addition, the expression of the *mttp* gene was significantly downregulated in both GLU and OA treated hepatocytes ($P < 0.05$) (Fig. 4D). The expression of the *adrp* gene was significantly downregulated in GLU treated hepatocytes and upregulated in OA treated hepatocytes ($P < 0.05$) (Fig. 4E).

3.6. Protein expression related to ER stress and lipid metabolism

Protein expression related to ER stress and lipid metabolism was measured using western blot (Fig. 5A). We found that GRP78 protein and IRE1 phosphorylation levels were increased only in fish administered HLD compared with those fed with CD ($P < 0.05$) (Fig. 5B–C). Similarly, ADRP protein level was increased only in fish administered HLD compared with those fed with CD ($P < 0.05$) (Fig. 5D). However, MTTP protein level was decreased only in fish administered HLD compared with those fed with CD ($P < 0.05$) (Fig. 5E).

4. Discussion

Fish is one of the necessities promoted by the Mediterranean diet. More than half of fish consumption in the world comes from aquaculture and therefore more attention has been paid to aquaculture (Willmann et al., 2009). Due to the higher protein demand, aquatic feed costs are much higher than that of livestock (Lall and Dumas, 2015). Protein raw materials, such as fishmeal and soybean meal, are expensive and in unstable supply. High carbohydrate diet and high lipid diet have been extensively used in the modern aquaculture industry (A et al., 2021; Ning et al., 2023; Yin et al., 2021). Increasing the levels of carbohydrates and lipids in the diet will promote fish growth within the optimal range. However, exceeding certain limits will result in excessive lipid deposition in the fish body (Gaylord and Iii, 2000; Liu et al., 2021). In the present study, our results showed that HCD and HLD did not affect the growth performance of fish, even though those two experimental diets contain higher energy density compared to CD. We speculate that fish can adjust their feeding profile to adapt to the energy of the diet as a way to meet maximum growth. Similar results have been verified for other fish species, such as *Oreochromis niloticus* (Wang et al., 2022), *Dicentrarchus labrax* (Peres and Oliva-Teles, 1999), *Nile tilapia* (Haidar et al., 2018), *Rachycentron canadum* (Wang et al., 2005).

The liver is the most critical metabolic organ of the organism. A high-calorie diet can easily lead to a series of liver metabolic diseases, such as diabetes mellitus and nonalcoholic fatty liver disease (NAFLD) (Huang et al., 2023; Nota et al., 2023). Due to the use of excessive carbohydrates

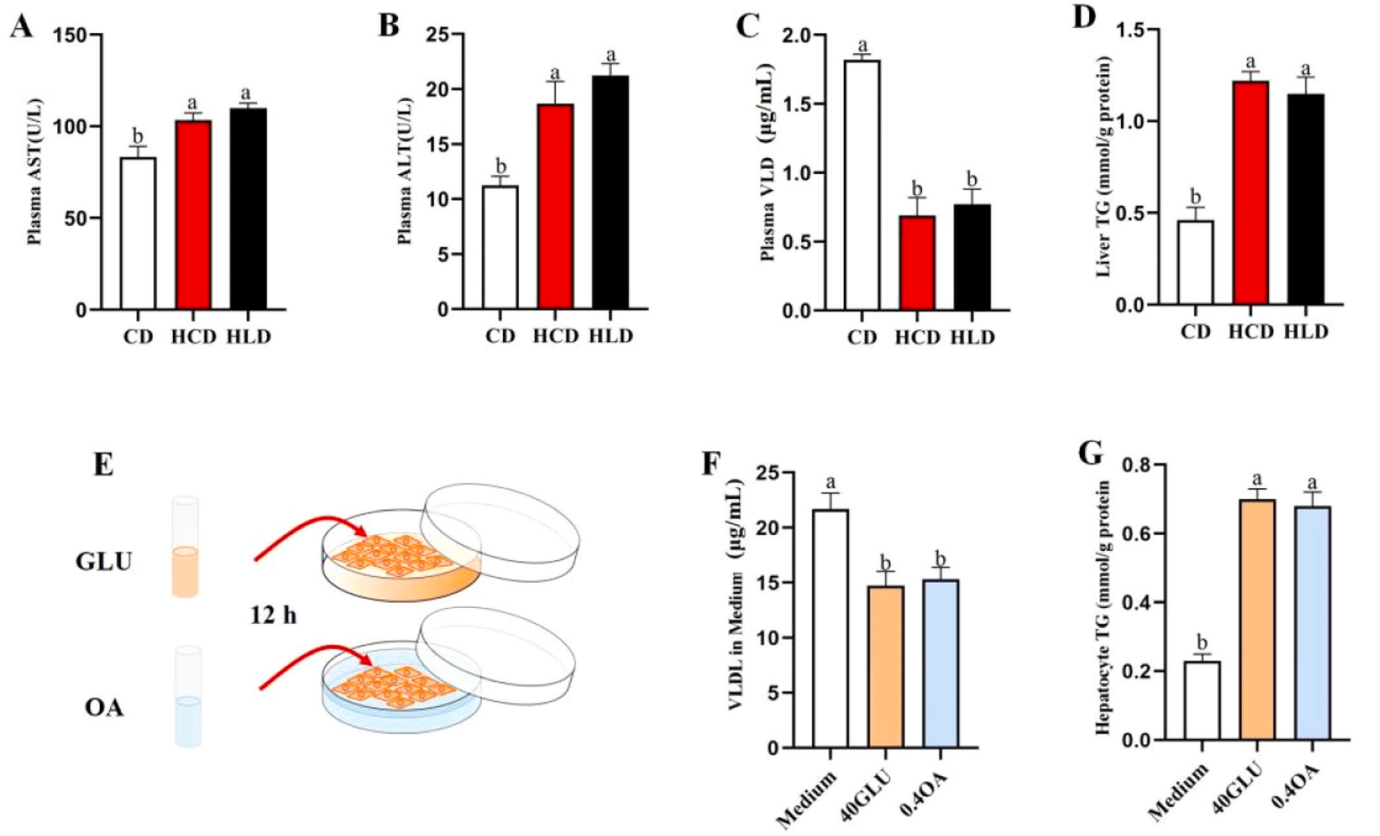

Fig. 1. Biochemical parameters of lipid metabolism *in vivo* and *in vitro*. (A-B) Enzyme activities of AST and ALT in plasma. (C) VLDL content in plasma. (D) Liver TG content. (E) Culture and treatment of primary hepatocytes of *Megalobrama megalobrama*. (F) VLDL content in medium. (G) Hepatocyte TG content. Data were presented as mean ± SEM (one-way ANOVA, n = 4). Values in bars that share the same superscript letter were not significantly different among treatments ($P > 0.05$). AST, Aspartate aminotransferase; ALT, Alanine aminotransferase; VLDL, Very low-density lipoprotein; TG, Triglycerides.

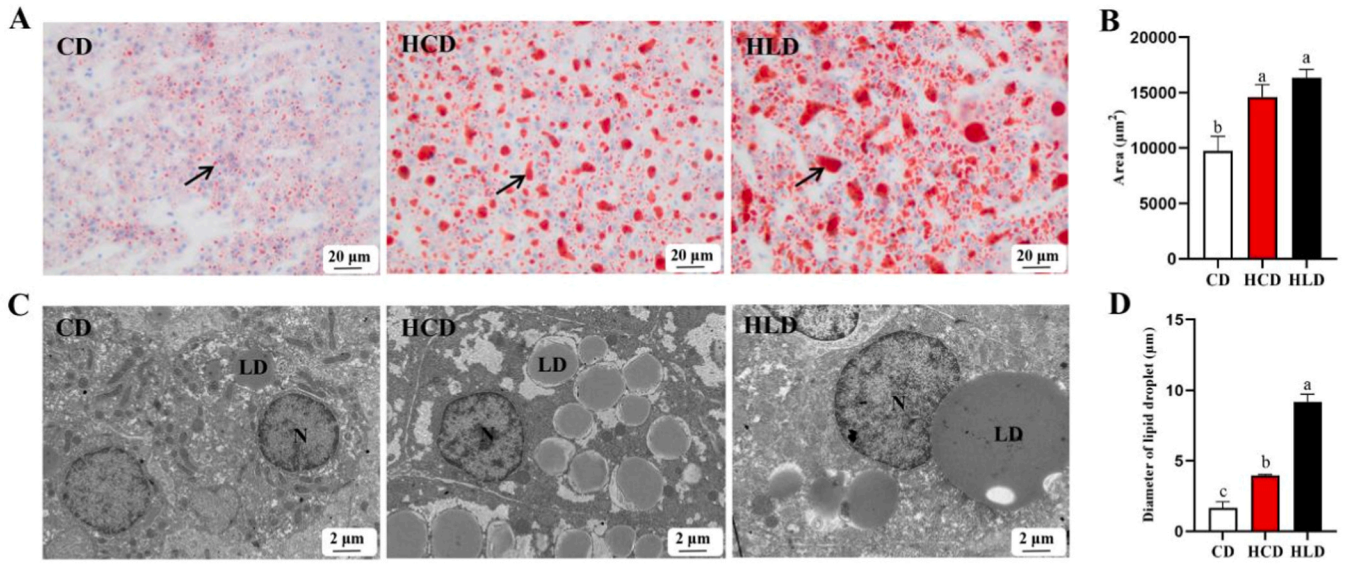

Fig. 2. Observation and analysis of liver morphology and ultrastructure of hepatocytes. (A) Oil red O staining of liver tissue from fish fed with the experimental diets (Scale bars, 20 μm). Red represents neutral lipids (The black arrow) and blue represents the nucleus. (B) The area of the stained neutral lipids was analyzed using Image J Pro 1.52 software (National Institutes of Health, Bethesda, USA). (C) Transmission electron microscope images of *Megalobrama amblycephala* hepatocytes (N, Nucleus; LD, Lipid droplet; Scale bars, 2 μm). (D) The diameter of lipid droplet was analyzed using Image J Pro 1.52 software (National Institutes of Health, Bethesda, USA). Data were presented as mean ± SEM (one-way ANOVA, n = 4). Values in bars that share the same superscript letter were not significantly different among treatments ($P > 0.05$).

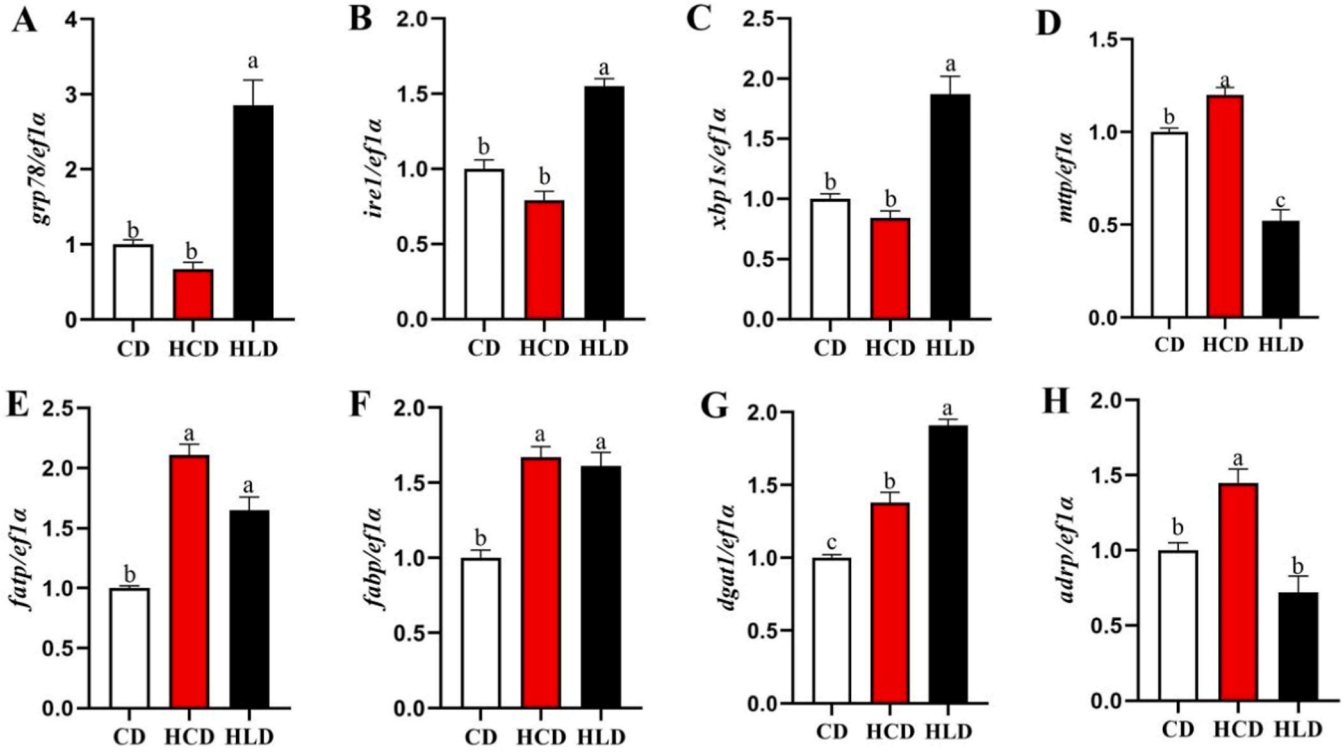

Fig. 3. The relative gene expression in the liver of *Megalobrama megalobrama* fed with the experimental diets. (A) *grp78*, glucose regulated protein 78. (B) *ire1*, inositol requiring enzyme 1. (C) *xbp1s*, spliced X box-binding protein 1. (D) *mttp*, microsomal triglyceride transfer protein. (E) *fatp*, fatty acid transport protein. (F) *fabp*, fatty acid binding protein. (G) *dgat1*, diacylglycerol acyltransferase 1. (H) *adrp*, adipose differentiation-related protein. Data were presented as mean ± SEM (one-way ANOVA, n = 4). Values in bars that share the same superscript letter were not significantly different among treatments ($P > 0.05$).

and lipids in aquatic feed to save protein, fish can develop symptoms of fatty liver. In line with previous studies, oil red O staining directly indicated that excess lipids and carbohydrates in the diet caused excessive deposition of lipids in the liver. Lipid metabolism in the liver is a very complex process, which includes fatty acid uptake, transport, β-oxidation, and lipoprotein secretion. VLDL is the main carrier of lipid secretion from the liver to peripheral tissues, and 60 % of a mature VLDL particle is composed of triglycerides. Decreased serum levels of VLDL indicate impairment of the liver's ability to secrete TG into peripheral tissues. We also confirmed this by further testing TG contents in the liver.

Studies in many species, including mice and fish, have demonstrated that deposition of liver lipids contributes to the development of endoplasmic reticulum stress, which in turn exacerbates impaired VLDL secretion (Cao et al., 2019; Ota et al., 2008). Our study states that HCD and HLD increased the mRNA expressions of *fatp, fabp,* and *dgat1*. These results suggest that both HCD and HLD promote lipogenesis in fish. The microsomal triglyceride transfer protein (MTTP) promotes the formation of VLDL precursors and transports TG to VLDL (Barrett et al., 2014; Fisher et al., 2011; Magkos et al., 2007). In the present study, the liver of fish fed with HLD showed a lower *mttp* mRNA expressions and protein levels. This result suggests a decrease in the formation of VLDL precursors and an abnormal secretion of hepatic lipids. As a result, we further explored the endoplasmic reticulum stress-related IRE1/XBP1 signaling pathway. GRP78 is recognized as a marker of endoplasmic reticulum stress. In the absence of stress, GRP78 binds to IRE1 to maintain cellular homeostasis. Accumulation of unfolded/misfolded proteins in the ER leads to the isolation of IRE1 from GRP78 (Aksoy et al., 2017; Chen et al., 2014; Yuan et al., 2021). IRE1 activates unconventional splicing of XBP1, leading to the production of the active transcription factor *xbp1* (Tam et al., 2014). It was found that HLD significantly increased the mRNA expressions and protein levels of *grp78* and *xbp1s*, as well as the phosphorylation of IRE1. This is also consistent with previous studies, namely that HLD activates the IRE1/XBP1 signaling pathway, which in turn impairs the ability to secrete VLDL of the liver. Our finding that HLD-induced ER stress impairs VLDL secretion aligns with Fang et al. (2021), who reported PKCδ-mediated VLDL inhibition in high-fat-fed *Larimichthys crocea*. However, while Fang et al. implicated oxidative stress as the primary driver, we demonstrated that ER stress (via IRE1/XBP1) was the dominant pathway in *M. amblycephala*. This divergence may reflect species-specific metabolic adaptations between marine carnivores and freshwater herbivores. It was also found in this study that HCD did not activate the endoplasmic reticulum stress-associated IRE1/XBP1 pathway, and in order to further validate the current results, in vitro experiments were performed. We carried out cultures of primary hepatocytes of the *Megalobrama amblycephala*, OA was used as a lipid source and D-Glucose as a carbohydrate source. The results showed that the content of TG in hepatocytes after treatment with 0.4 OA and 40 D-glucose was significantly increased and the content of VLDL in the supernatant was significantly decreased. This is also consistent with the results of the feeding trial.

The large amount of TG required for lipidation and maturation of VLDL can come directly from lipid droplets. Lipid droplets, as very active subcellular structures, have a variety of lipid droplet proteins distributed on them (Barneda et al., 2013). It promotes the fusion and growth of lipid droplets. PAT family proteins are another well-studied family of proteins localized to lipid droplets, including ADRP (Adipose Differentiation Related Protein), which also plays an important role in the metabolism of lipid droplets (Egan et al., 1990). Interestingly, knockdown of ADRP in the hepatocytes then results in larger lipid droplets (Lee et al., 2010). This phenomenon suggests that ADRP inhibition promotes the fusion of lipid droplets. Transmission electron microscopy of hepatocytes showed that the number of lipid droplets in the HCD group became more. Individual lipid droplets in the HLD group were larger. Transcript levels of ADRP also explain this phenomenon.

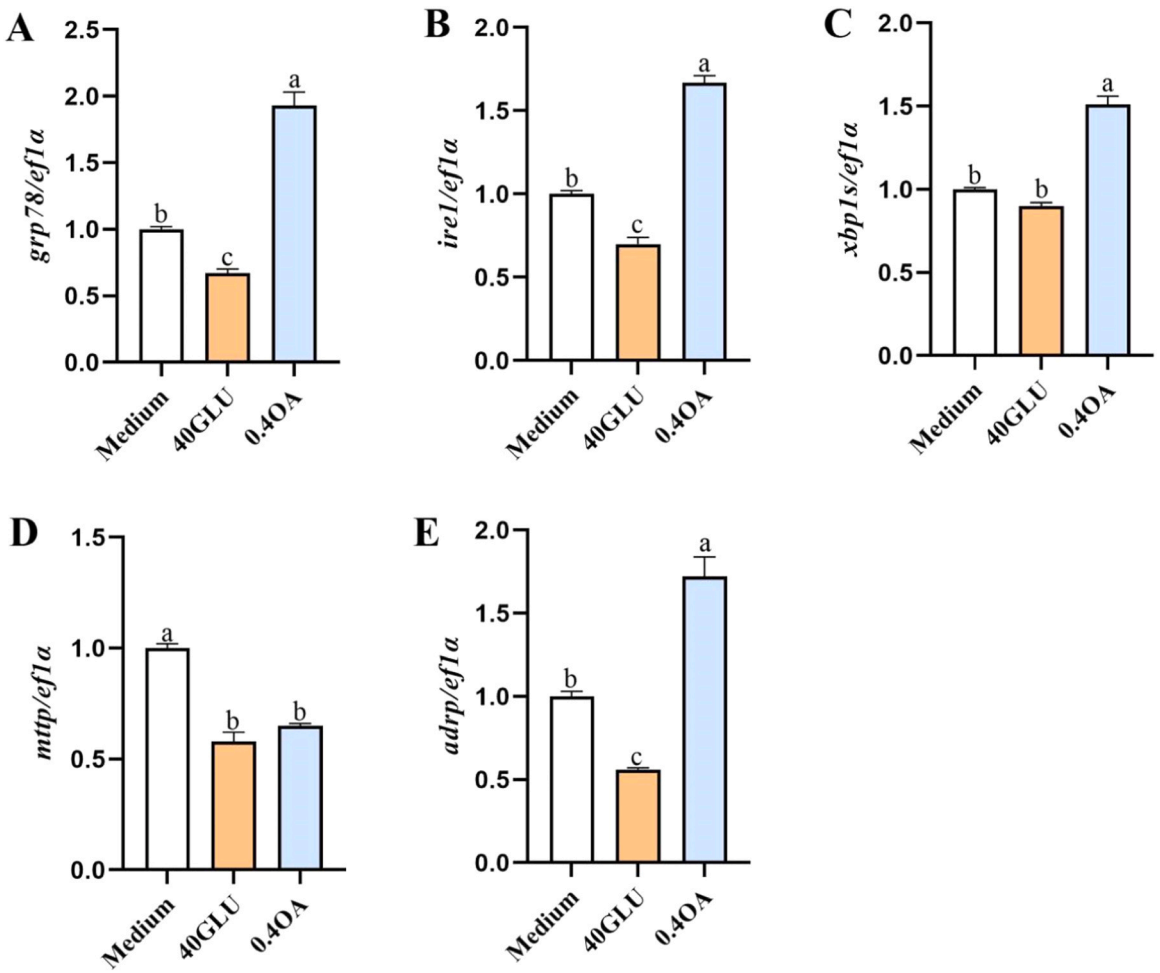

Fig. 4. The relative gene expression in hepatocytes exposed to 40 mM D-glucose (GLU) and 0.4 mM oleic acid (OA) for 12 h. (A) *grp78*, glucose regulated protein 78. (B) *ire1*, inositol requiring enzyme 1. (C) *xbp1s*, spliced X box-binding protein 1. (D) *mttp*, microsomal triglyceride transfer protein. (E) *adrp*, adipose differentiation-related protein. Data were presented as mean ± SEM (one-way ANOVA, n = 4). Values in bars that share the same superscript letter were not significantly different among treatments ($P > 0.05$).

5. Conclusion

Collectively, chronic exposure to hyperglycemic and high-lipid diets promotes excessive hepatic lipid deposition in fish, ultimately inducing hepatic steatosis. The high-carbohydrate diets facilitate lipogenesis through the upregulation of de novo lipid synthesis pathways, thereby increasing the number of lipid droplets (microsteatosis). In contrast, the high-lipid diets predominantly impair VLDL assembly and secretion via ER stress-mediated mechanisms, leading to ectopic lipid accumulation. Concomitantly, the formation of macrosteatosis under high-lipid conditions may serve as a cytoprotective adaptation to mitigate hepatic metabolic stress. These findings demonstrate that both hyperenergetic dietary regimens differentially compromise fish hepatic homeostasis through distinct pathophysiological mechanisms.

Author statement

We declare that this manuscript is original, has not been published before and is not currently being considered for publication elsewhere. We confirm that the manuscript has been read and approved by all named authors and that there are no other persons who satisfied the criteria for authorship but are not listed. We further confirm that the order of authors listed in the manuscript has been approved by all of us.

Data sharing

Data available on request from the authors.

CRediT authorship contribution statement

Xiaoyu Chu: Methodology, Investigation. **Xi Wang:** Visualization, Methodology. **Yangyang Huang:** Visualization, Methodology, Investigation, Data curation. **Xiufei Cao:** Writing – original draft, Investigation, Funding acquisition, Data curation, Conceptualization. **Wenbin Liu:** Supervision, Funding acquisition, Conceptualization. **jiang guangzhen:** Writing – review & editing, Supervision, Conceptualization. **Xiaoe Xiang:** Methodology, Investigation. **Linghong Miao:** Investigation, Funding acquisition. **Sunyuan Zheng:** Investigation, Formal analysis, Data curation. **Xiaoli Shi:** Methodology, Investigation.

Funding

This research was supported by the National Key Research and Development Plan Program of China (2022YFD2400600/2022YFD2400603), China Postdoctoral Science Foundation (2024M751453), and Jiangsu Natural Science Foundation for basic research (BK20201325).

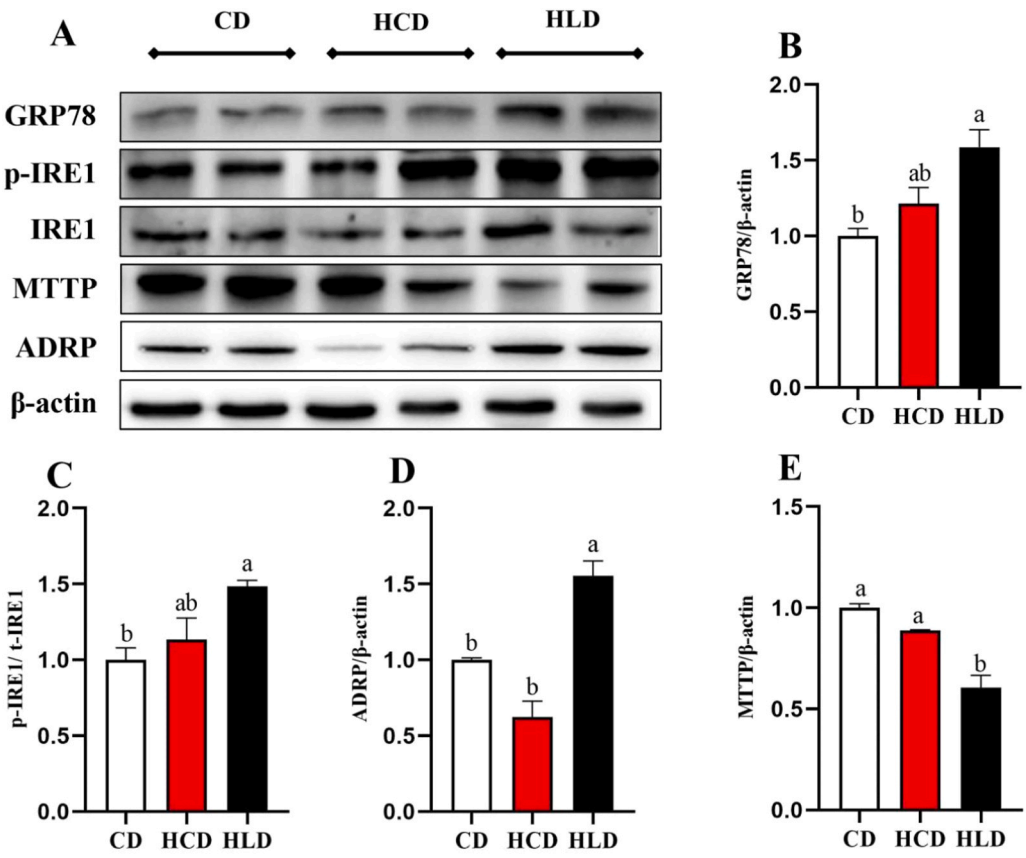

Fig. 5. Western blot analysis of proteins in the liver from *Megalobrama megalobrama* fed with the experimental diets. (A) Western blot of GRP78, p-IRE1, IRE1, MTTP, ADRP, and β-actin. (B-E) The protein expressions of GRP78, p-IRE1, ADRP, and MTTP were analyzed using Image J Pro 1.52 software (National Institutes of Health, Bethesda, USA). The protein expression levels of GRP78, ADRP, and MTTP were normalized to β-actin as an internal control, while phosphorylated IRE1 (p-IRE1) levels were expressed relative to total IRE1 protein. Data were presented as mean ± SEM (one-way ANOVA, n = 4). Values in bars that share the same superscript letter were not significantly different among treatments ($P > 0.05$). GRP78, Glucose regulated protein 78; p-IRE1, Phosphorylated inositol requiring enzyme 1; IRE1, Inositol requiring enzyme 1; ADRP, Adipose differentiation-related protein; MTTP, Microsomal triglyceride transfer protein.

Declaration of Competing Interest

The authors declare that they have no known competing financial interests or personal relationships that could have appeared to influence the work reported in this paper.

Data availability

Data will be made available on request.

References

A, Y.L., A, S.L., A, Y.S., B, Y.L., C, C.C.A., D, C.Y., et al., 2021. Impacts of dietary konjac glucomannan supplementation on growth, antioxidant capacity, hepatic lipid metabolism and inflammatory response in golden pompano (Trachinotus ovatus) fed a high fat diet. Aquaculture.

Aksoy, M.O., Kim, V., Cornwell, W.D., Rogers, T.J., Kosmider, B., Bahmed, K., et al., 2017. Secretion of the endoplasmic reticulum stress protein, grp78, into the balf is increased in cigarette smokers. Respir. Res. 18.

Barneda, D., Frontini, A., Cinti, S., Christian, M., 2013. Dynamic changes in lipid droplet-associated proteins in the "browning" of White adipose tissues. Biochim. Et. Biophys. ActaMol. Cell Biol. Lipids 1831 (5), 924–933.

Barrett, P., H, R., Wong, A., et al., 2014. Association between skeletal muscle fat content and very-low-density lipoprotein-apolipoprotein b-100 transport in obesity: effect of weight loss. Diabetes Obes. Metab.

Boujard, T., Gélineau, A., Covès, D., Corraze, G., Dutto, G., Gasset, E., et al., 2004. Regulation of feed intake, growth, nutrient and energy utilisation in european sea bass (*Dicentrarchus labrax*) fed high fat diets. Aquaculture 231 (1-4), 529–545.

Cao, X.-F., Dai, Y.-J., Liu, M.-Y., Yuan, X.-Y., Wang, C.-C., Huang, Y.-Y., et al., 2019. High-fat diet induces aberrant hepatic lipid secretion in blunt snout bream by activating endoplasmic reticulum stress-associated ire1/xbp1 pathway. Biochim. Et. Biophys. ActaMol. Cell Biol. Lipids 1864 (3), 213–223.

Chen, Q., Fang, W., Shen, Y., Xu, D., Chen, Q., Cui, K., et al., 2022. Suppression of cideb under endoplasmic reticulum stress exacerbated hepatic inflammation by inducing hepatic steatosis and oxidative stress. Free Radic. Biol. Med. 18567–18575.

Chen, L., Xu, S., Liu, L., Wen, X., Xu, Y., Chen, J., et al., 2014. Cab45s inhibits the er stress-induced ire1-jnk pathway and apoptosis via grp78/bip. Cell Death Dis. 5.

Dong, Y., Wang, X., Wei, L., Liu, Z., Chu, X., Xiong, W., et al., 2024. The effectiveness of four nicotinamide adenine dinucleotide (nad^{+}) precursors in alleviating the high-glucose-induced damage to hepatocytes in megalobrama amblycephala: evidence in nad^{+} homeostasis, sirt1/3 activation, redox defense, inflammatory response, apoptosis, and glucose metabolism. Antioxidants 13 (4).

Egan, J.J., Greenberg, A.S., Chang, M.K., Londos, C., 1990. Control of endogenous phosphorylation of the major camp-dependent protein-kinase substrate in adipocytes by insulin and beta-adrenergic stimulation. J. Biol. Chem. 265 (31), 18769–18775.

Fang, W., Chen, Q., Cui, K., Chen, Q., Li, X., Xu, N., et al., 2021. Lipid overload impairs hepatic vldl secretion via oxidative stress-mediated pkcs-hnf4α-mtp pathway in large yellow croaker (*Larimichthys crocea*). Free Radic. Biol. Med. 172213–172225.

Fisher, E.A., 2012. The degradation of apolipoprotein b100: multiple opportunities to regulate vldl triglyceride production by different proteolytic pathways. Biochim. Et. Biophys. ActaMol. Cell Biol. Lipids 1821 (5), 778–781.

Fisher, E.A., Khanna, N.A., Mcleod, R.S., 2011. Ubiquitination regulates the assembly of vldl in hepg2 cells and is the committing step of the apob-100 erad pathway. J. Lipid Res. 52 (6), 1170.

Gaylord T.G., Iii D.M.G.. Dietary lipid level but not l-carnitine affects growth performance of hybrid striped bass (Morone chrysops ♀×m. Saxatilis ♂), 2000;190 (3-4):0-246.

Haidar, M.N., Bleeker, S., Heinsbroek, L.T.N., Schrama, J.W., 2018. Effect of constant digestible protein intake and varying digestible energy levels on energy and protein utilization in Nile tilapia. Aquaculture 48928–48935.

Huang, Y.-y, Jiang, G.-z, Abasubong, K.P., Wang, C.-c, Zhang, L., Dai, Y.-j, et al., 2022. High lipid and high carbohydrate diets affect muscle growth of blunt snout bream (*Megalobrama amblycephala*) through different signaling pathways. Aquaculture 548.

Huang, C., Tan, H., Song, M., Ke, Liu, Hongbin, Wang, Jun, Shi, Yanqiang, Hou, Fengyi, Zhou, Qian, Huang, Ruo, Shen, Binghai, Lin, Xinlong, Qin, Xiaoming, Zhi, Fachao, 2023. Maternal Western diet mediates susceptibility of offspring to crohn's-like colitis by deoxycholate generation. microbiome 11 (1).

Karavia, E.A., Papachristou, D.J., Kotsikogianni, I., Triantafyllidou, I.-E., Kypreos, K.E., 2013. Lecithin/cholesterol acyltransferase modulates diet-induced hepatic deposition of triglycerides in mice. J. Nutr. Biochem. 24 (3), 567–577.
Lall, S.P., Dumas, A., 2015. Nutritional requirements of cultured fish: formulating nutritionally adequate feeds - sciencedirect. Feed. Feed. Pract. Aquac. 53–109.
Lee, T.F., Mak, K.M., Rackovsky, O., Lin, Y.-L., Kwong, A.J., Loke, J.C., et al., 2010. Downregulation of hepatic stellate cell activation by retinol and palmitate mediated by adipose differentiation-related protein (adrp). J. Cell. Physiol. 223 (3), 648–657.
Li, X.-f, Liu, W.-b, Jiang, Y.-y, Zhu, H., Ge, X.-p, 2010. Effects of dietary protein and lipid levels in practical diets on growth performance and body composition of blunt snout bream (*Megalobrama amblycephala*) fingerlings. Aquaculture 303 (1-4), 65–70.
Li, X., Ye, J., Zhou, L., Gu, W., Fisher, E.A., Li, P., 2012. Opposing roles of cell death-inducing dff45-like effector b and perilipin 2 in controlling hepatic vldl lipidation. J. Lipid Res. 53 (9), 1877–1889.
Liu, G., Yu, H., Wang, C., Li, P., Liu, S., Zhang, X., et al., 2021. Nanoselenium supplements in high-fat diets relieve hepatopancreas injury and improve survival of grass carp ctenopharyngodon idella by reducing lipid deposition. Aquaculture 538 (000).
Lu, K.-L., Xu, W.-N., Li, X.-F., Liu, W.-B., Wang, L.-N., Zhang, C.-N., 2013. Hepatic triacylglycerol secretion, lipid transport and tissue lipid uptake in blunt snout bream (*Megalobrama amblycephala*) fed high-fat diet. Aquaculture 408160–408168.
Magkos, F., Patterson, B.W., Mohammed, B.S., Mittendorfer, B., 2007. A single 1-h bout of evening exercise increases basal ffa flux without affecting vldl-triglyceride and vldl-apolipoprotein b-100 kinetics in untrained lean men. Am. J. Physiol. Endocrinol. Metab. 292 (6), E1568–E1574.
Mizuta, D.D., Froehlich, H.E., Wilson, J.R., 2022. The changing role and definitions of aquaculture for environmental purposes. Rev. Aquac.
Naylor, R.L., Hardy, R.W., Bureau, D.P., Chiu, A., Elliott, M., Farrell, A.P., et al., 2009. Feeding aquaculture in an era of finite resources (vol 106, 15103, 2009). Proc. Natl. Acad. Sci. 106 (42), 18040-18040.
Ning, L., Zhang, H., Chen, X., Zhen, J., Chen, S., Guang, J., et al., 2023. A comparative study on the tolerance of tilapia (Oreochromis niloticus)to high carbohydrate and high lipid diets. Anim. Nutr. 2, 160–172.
Nota, M., Nicolas, S., O'Leary, O., Nolan, Y., 2023. Outrunning a bad diet: interactions between exercise and a Western-style diet for adolescent mental health, metabolism and microbes. Neurosci. Biobehav. Rev. 149.
Ota, T., Gayet, C., Ginsberg, H.N., 2008. Inhibition of apolipoprotein b100 secretion by lipid-induced hepatic endoplasmic reticulum stress in rodents. J. Clin. Investig. 118 (1).
Peres, H., Oliva-Teles, A., 1999. Effect of dietary lipid level on growth performance and feed utilization by european sea bass juveniles (*Dicentrarchus labrax*). Aquaculture 179 (1-4), 325–334.
Spaulding, S.C., Choudhary, V., Bollag, W.B., 2023. Phospholipase d mediates very low-density lipoprotein-induced aldosterone production, in part, via lipin-1. J. Mol. Endocrinol. 70 (4).
Taagepera, R., Nemcok, M., 2024. World population growth over millennia: ancient and present phases with a temporary halt in-between. Anthr. Rev. 11 (1), 163–183.
Tacon, A.G.J., Metian, M., 2018. Food matters: fish, income, and food supply-a comparative analysis. Rev. Fish. Sci. Aquac. 26 (1), 15–28.
Tam, A.B., Koong, A.C., Niwa, M., 2014. Ire1 has distinct catalytic mechanisms for xbp1/hac1 splicing and ridd. Cell Rep. 9 (3), 850–858.
Tveteras, S., Asche, F., Bellemare, M.F., Smith, M.D., Guttormsen, A.G., Lem, A., et al., 2012. Fish is food - the fao's fish price index. Plos One 7 (5).
Wang, K.-W., Chen, J.-X., Liu, Q.-Q., Deng, X., Luo, L., Lin, S.-M., et al., 2022. A comparison between high carbohydrate and high lipid diets reception on the growth, feed utilization and glucose homeostasis of genetically improved farmed tilapia oreochromis niloticus. Aquac. Rep. 24.
Wang, J.T., Liu, Y.J., Tian, L.X., Mai, K.S., Du, Z.Y., Wang, Y., et al., 2005. Effect of dietary lipid level on growth performance, lipid deposition, hepatic lipogenesis in juvenile cobia (*Rachycentron canadum*). Aquaculture 249 (1-4), 439–447.
Watanabe, T., 1982. Lipid nutrition in fish. Comp. Biochem. Physiol. Part B Comp. Biochem. 73 (1), 3–15.
Willmann, R., Cochrane, K.L., Emerson, W., 2009. Fao guidelines for ecolabelling in wild-capture fisheries. Seaf. Ecolabelling Princ. Pract.
Xie, D., Yang, L., Yu, R., Chen, F., Lu, R., Qin, C., et al., 2017. Effects of dietary carbohydrate and lipid levels on growth and hepatic lipid deposition of juvenile tilapia, *Oreochromis niloticus*. Aquaculture 479696–479703.
Ye, J., Li, J.Z., Liu, Y., Li, X., Yang, T., Ma, X., et al., 2009. Cideb, an er- and lipid droplet-associated protein, mediates vldl lipidation and maturation by interacting with apolipoprotein b. Cell Metab. 9 (2), 177–190.
Yin, P., Xie, S., Zhuang, Z., He, X., Tang, X., Tian, L., et al., 2021. Dietary supplementation of bile acid attenuate adverse effects of high-fat diet on growth performance, antioxidant ability, lipid accumulation and intestinal health in juvenile largemouth bass (Micropterus salmoides). Aquaculture 531 (000).
Yuan, J., Yao, C., Tang, J., Liu, Y., Huang, C., Yu, S., et al., 2021. Enhanced grp78 protein expression via the ire1α/ask1/p38 mapk pathway during as_2o_3-induced endoplasmic reticulum stress in beas-2b cells. Toxicology 462.
Zhong, C., Feng, Y., Xu, Y., 2023. Production of fish analogues from plant proteins: potential strategies, challenges, and outlook. Foods 12 (3).